




In the format provided by the authors and unedited.

Cumulus provides cloud-based data analysis for large-scale single-cell and single-nucleus RNA-seq

Bo Li ^{1,2,3} , Joshua Gould ¹, Yiming Yang ^{1,2}, Siranush Sarkizova^{4,5}, Marcin Tabaka¹, Orr Ashenberg¹, Yanay Rosen¹, Michal Slyper¹, Monika S. Kowalczyk¹, Alexandra-Chloé Villani^{2,3,4,6}, Timothy Tickle¹, Nir Hacohen ^{3,4,6}, Orit Rozenblatt-Rosen ¹  and Aviv Regev ^{1,7,8,9} 

¹Klarman Cell Observatory, Broad Institute of Harvard and MIT, Cambridge, MA, USA. ²Division of Rheumatology, Allergy, and Immunology, Center for Immunology and Inflammatory Diseases, Massachusetts General Hospital, Boston, MA, USA. ³Department of Medicine, Harvard Medical School, Boston, MA, USA. ⁴Broad Institute of Harvard and MIT, Cambridge, MA, USA. ⁵Department of Biomedical Informatics, Harvard Medical School, Boston, MA, USA. ⁶Center for Cancer Research, Massachusetts General Hospital, Boston, MA, USA. ⁷Howard Hughes Medical Institute, Massachusetts Institute of Technology, Cambridge, MA, USA. ⁸Koch Institute of Integrative Cancer Research, Massachusetts Institute of Technology, Cambridge, MA, USA. ⁹Department of Biology, Massachusetts Institute of Technology, Cambridge, MA, USA. [✉]e-mail: bli28@mgh.harvard.edu; orit@broadinstitute.org; aregev@broadinstitute.org

Cumulus provides cloud-based data analysis for large-scale
single-cell and single-nucleus RNA-seq

Li B. et al.

Feature	Falco	Cumulus
Require local installation?	Yes	No
Friendly to biologists?	No, command line interface only	Yes, providing web-based GUI through Terra
Sc/snRNA-seq input modality	Plated-based SMART-seq2 only	Both plate-based and droplet-based
Support of CITE-seq, cell hashing, nucleus-hashing, or Perturb-seq?	No	Yes
Type of analysis supported?	Only gene-count matrix generation	FASTQ extraction, gene-count matrix generation and downstream analysis such as cell clustering and putative cell type annotation
Cloud platform	AWS	Google Cloud Platform, but generally cloud agnostic
Provide tools for visualization?	No	Yes, Cirrocumulus

Supplementary Table 1. Comparison of features provided by Falco and Cumulus.

Feature	Cumulus	Cell Ranger
Cloud-based	✓	
Web-based user interface	✓	
Web-based interactive visualization	✓	
Reads extraction (from sequencers)	✓	✓
Count matrix generation: Droplet-based data (10x v2 and v3)	✓	✓
Count matrix generation: Droplet-based data (Drop-seq)	✓	
Count matrix generation: Plated-based data (SMART-Seq2)	✓	
Biological analyses	✓	✓
CITE-seq	✓	✓
Cell hashing	✓	
Nucleus hashing	✓	
Perturb-seq	✓	✓

Supplementary Table 2. Comparison of features (rows) between Cumulus and Cell Ranger (columns).

Feature	Pegasus	Seurat v3	SCANPY
Quality control	✓	✓	✓
Highly variable gene selection	✓	✓	✓
Batch correction	✓	✓	✓
Data integration		✓	✓
PCA	✓	✓	✓
k nearest neighbor graph construction	✓	✓	✓
Diffusion map	✓		✓
Pseudotime calculation	✓		✓
Branching events detection			✓
Louvain-like clustering	✓	✓	✓
Leiden-like clustering	✓	✓	✓
tSNE-like visualization	✓	✓	✓
UMAP-like visualization	✓	✓	✓
FLE-like visualization	✓		✓
Gene signature scores		✓	✓
Differential expression analysis	✓	✓	✓
Classification-based marker detection	✓		
Marker-based cell type annotation	✓		
Imputation			✓
Simulation			✓
Label transfer		✓	

Supplementary Table 3. Comparison of features supported by Pegasus, Seurat v3 and SCANPY.

Analysis	Seurat v3	SCANPY	Pegasus
HVG selection	2 min, 7 s	1 min, 27 s	11 s
Batch correction	Failed after 5h, 39 min	8 min, 4 s	19 s
PCA	5 min, 47 s	12 s	11 s
Find k nearest neighbors	55 s	4 min, 43 s	15 sec
Diffusion map	n/a	4 min, 8 s	2 min, 47 s
Louvain-like clustering	9 min, 32 s	23 min, 48 s	1 min, 15 s
Leiden-like clustering	Failed	43 min, 22 s	1 min, 9s
tSNE-like visualization	3 min, 3 s	19 min, 2 s	2 min, 49 s
UMAP-like visualization	6 min, 28 s	5 min, 49 s	2 min, 24 s
FLE-like visualization	n/a	15 h, 36 min	15 min, 20 s

Supplementary Table 4. Execution time for 10 key analysis tasks on the bone marrow dataset by each tool. Every tool was run on a 28-thread, 256G memory server. Bold font: shortest execution time.

Analysis	SCANPY	Pegasus
HVG selection	3 min, 43 s	1 min, 50 s
Batch correction	1 h, 26 min	2 min, 18 s
PCA	57 s	57 s
Find k nearest neighbors	26 min, 10 s	1 min, 28 s
Diffusion map	28 min, 4 s	20 min, 13 s
Louvain-like clustering	1 h, 41 min	7 min, 10 s
Leiden-like clustering	15 h, 59 min	6 min, 24 s
tSNE-like visualization	1 h, 39 min	11 min, 48 s
UMAP-like visualization	36 min, 31 s	11 min, 28 s
FLE-like visualization	\approx 3 d 20 h	1 h, 38 min

Supplementary Table 5. Execution time for 10 key analysis tasks on the the 1.3 million mouse brain dataset by each tool. Every tool was run on a 28-thread, 256G memory server. Seurat v3 failed to load the big gene-count matrix and thus is omitted from the table. Bold font: shortest execution time.

Analysis	Seurat v3	SCANPY	Pegasus
HVG selection	3.15 s	1.83 s	0.18 s
PCA	7.49 s	0.25 s	0.18 s
Find k nearest neighbors	1.08 s	6.05 s	0.27 s
Diffusion map	n/a	0.81 s	1.11 s
Louvain-like clustering	2.58 s	2.56 s	1.53 s
Leiden-like clustering	19.01 s	6.14 s	4.14 s
tSNE-like visualization	25.00 s	12.82 s	27.97 s
UMAP-like visualization	19.98 s	11.75 s	7.81 s
FLE-like visualization	n/a	6 min 42 s	14.03 s

Supplementary Table 6. Execution time for 9 key analysis tasks on the 5K PBMC data by each tool, using only 8 threads. Every tool was run on a 28-thread, 256G memory server. But each tool only used 8 threads to mimic a laptop setting. Batch correction is not included because all cells are from a same batch. Bold font: shortest execution time.

Data	Seurat v3	SCANPY	Pegasus
5K PBMC	1.57 GB	1.03 GB	1.00 GB
Bone marrow	67.85 GB	16.81 GB	17.02 GB

Supplementary Table 7. Peak memory for running Seurat v3, SCANPY and Pegasus on the small 5K PBMC and large bone marrow datasets.

Tool	Execution Time	Cost
Cell Ranger	7 h 46 min	\$2.61
Optimus	16 h 1 min	\$18.43
Alevin	2 h 27 min	\$0.80
Kallisto-BUStools	42 min	\$0.28
STARsolo	58 min	\$0.29

Supplementary Table 8. Benchmarking Cell Ranger, Optimus, Alevin, Kallisto-BUStools and STARsolo on 5K human PBMC data using cloud. Execution time and computational costs are listed in the 2nd and 3rd columns respectively.

1 Supplementary Note 1

1.1 Preprocessing

The preprocessing step consists of 5 subtasks: *making gene symbols unique*, *selecting high quality cells*, *selecting robust genes*, *generating optional quality control reports*, and *transforming counts into log expression values*.

Making gene symbols unique. Pegasus takes a gene-by-cell count matrix as input. In this matrix, each gene is represented by a gene symbol. However, it is possible that multiple genes have a same gene symbol. To make sure each gene has a unique gene symbol, Pegasus appends suffix strings to genes with duplicated gene symbols. In particular, suppose that genes $1, \dots, n$ have the same gene symbol “sym”. Pegasus will transform gene i ’s gene symbol from “sym” to “sym.($i - 1$)” for $i \geq 2$. (e.g. gene 2’s symbol is “sym.1”).

Selecting high quality cells. Pegasus enables users to select high quality cells based on a combination of the following criteria: (1) number of detected genes (with at least 1 Unique Molecular Identifier (UMI)) $\geq \text{min_genes}$; (2) number of detected genes $< \text{max_genes}$; (3) number of total UMIs $\geq \text{min_umis}$; (4) number of total UMIs $< \text{max_umis}$; (5) percentage of UMIs from mitochondrial genes $< \text{percent_mito}$. min_genes , max_genes , min_umis , max_umis , and percent_mito are user-defined parameters.

Selecting robust genes. Genes that are only detected by a small portion of cells might correspond to random noise. Thus Pegasus identifies a set of robust genes which are detected in at least x percent of total cells. Pegasus selects variable genes only from the robust gene set. x is a user-defined parameter. The default value is $x = 0.05\%$, which corresponds to 3 cells out of 6,000 cells.

Generating optional quality control reports. Pegasus can generate optional quality control reports as Excel spreadsheets and PDF figures.

The spreadsheet contains two tabs — **Cell filtration stats** and **Gene filtration stats**. **Cell filtration stats** tab contains 10 columns: **Channel**, **kept**, **median_n_genes**, **median_n_umis**, **median_percent_mito**, **filt**, **total**, **median_n_genes_before**, **median_n_umis_before**, and **percent_mito_before**. **Channel** lists names for channels included in the input data. **kept** lists the number of high quality cells each channel keeps. **median_n_genes**, **median_n_umis**, and **median_percent_mito** list the median number of detected genes, median number of UMIs and median percentage of mitochondrial UMIs among high quality cells for each channel. **filt** lists the number of low quality cells filtered out for each channel. **total** lists the total number of cells before filtration. **median_n_genes_before**, **median_n_umis_before**, and **percent_mito_before** list the median number of detected genes, median number of UMIs and median percentage of mitochondrial UMIs for each channel before filtration. **Gene filtration stats** tab has 3 columns: **gene**, **n_cells**, and **percent_cells**. **gene** lists gene symbols for all non-robust genes. **n_cells** lists the number of high quality cells each gene is detected. **percent_cells** lists the percentage of high quality cells having the gene detected. Genes are sorted in descending order with respect to **n_cells**.

Pegasus can also generate split violin plots in PDF format to compare the distribution of detected genes, total UMIs, or percentage of mitochondrial UMIs between high quality cells and all cells.

Transforming counts into log expression values. Because different cells are sequenced in different depth, we need to normalize each single cell so that their expression profiles are comparable [14]. Suppose we have G genes in total and R represents the set of robust genes. For a cell with UMI count vector (c_1, \dots, c_G) , Pegasus multiplies a factor α to it to yield the normalized expression levels, (y_1, \dots, y_G) :

$$(y_1, \dots, y_G) = \alpha \cdot (c_1, \dots, c_G), \quad \text{such that } \sum_{i \in R} \alpha c_i = c,$$

where c is a user-defined constant. The default value is $c = 100,000$, which leads to expression levels in TP100K (transcripts per 100K).

Pegasus then transforms normalized expressions (y_1, \dots, y_G) into the log space. The log expression values (Y_1, \dots, Y_G) are calculated as follows:

$$Y_g = \log(y_g + 1). \tag{1}$$

1.2 Highly variable gene selection

Highly variable gene (HVG) selection is a common feature selection step for scRNA-Seq data analysis. This step selects a set of informative genes showing higher than expected variances in their expression levels. Once we select HVGs, we perform all downstream analyses on these HVGs only.

Pegasus selects HVGs only among robust genes R and implements two styles of selecting HVGs: Pegasus and Seurat.

1.2.1 Pegasus style

We conduct all downstream analyses, such as dimension reduction and clustering, on the log expression space. It is natural to wonder why we do not select HVGs on the log expression space as well? Thus, Pegasus implements a simple HVG selection procedure directly on the log expression space.

HVG selection in log expression space. Suppose we have N cells in total, we first calculate means and variances in the log space as follows for all genes in R :

$$\begin{aligned}\hat{\mu}_g &= \frac{1}{N} \sum_{i=1}^N Y_{ig}, \\ \hat{\sigma}_g^2 &= \frac{1}{N-1} \sum_{i=1}^N (Y_{ig} - \hat{\mu}_g)^2.\end{aligned}$$

We then fit a LOESS curve [3] of degree 2 between the means and variances (Supplementary Fig. 1a) using scikit-misc [9] Python package. We set the span parameter to 0.02. We denote LOESS-predicted variance for gene g as $\tilde{\sigma}_g^2$ and we know that any gene g with $\hat{\sigma}_g^2 > \tilde{\sigma}_g^2$ has a higher-than-expected variance.

There are two ways of ranking genes with higher-than-expected variances: by difference and by fold change. Let

$$\delta_g = \hat{\sigma}_g^2 - \tilde{\sigma}_g^2 \quad \text{and} \quad \tau_g = \frac{\hat{\sigma}_g^2}{\tilde{\sigma}_g^2}.$$

We rank each robust gene in R in descending order with respect to δ_g and τ_g respectively and denote its rankings as $rank_\delta(g)$ and $rank_\tau(g)$. We then define the overall ranking of a gene as the sum of its two rankings to combine the strengths of the two ranking methods:

$$rank(g) = rank_\delta(g) + rank_\tau(g).$$

HVGs are selected as the top n genes according to $rank(g)$, where $n = 2000$ by default.

Remove variance due to batch effects. Batch effects are technical noises added to our data during the processes of sample handling, library preparation, and sequencing. We do not want batch effects to participate in the HVG selection procedure and thus need to come up a way to remove variances due to batch effects before we fit the LOESS curve.

Suppose we have K biologically different groups, each group k contains n_k batches and each batch j contains n_{kj} cells. The total number of cells $N = \sum_{k=1}^K \sum_{j=1}^{n_k} n_{kj}$ and the mean and variance of each gene g become

$$\begin{aligned}\hat{\mu}_g &= \frac{1}{N} \sum_{k=1}^K \sum_{j=1}^{n_k} \sum_{i=1}^{n_{kj}} Y_{kji g}, \\ \hat{\sigma}_g^2 &= \frac{1}{N-1} \sum_{k=1}^K \sum_{j=1}^{n_k} \sum_{i=1}^{n_{kj}} (Y_{kji g} - \mu_g)^2.\end{aligned}$$

Based on the equations below, we can decompose the variance of gene g ($\hat{\sigma}_g^2$) into three components: variance within batches ($\hat{\sigma}_{g1}^2$), variance between batches ($\hat{\sigma}_{g2}^2$) and variance between biological groups ($\hat{\sigma}_{g3}^2$).

$$\begin{aligned}
\hat{\sigma}_g^2 &= \frac{1}{N-1} \sum_{k=1}^K \sum_{j=1}^{n_k} \sum_{i=1}^{n_{kj}} ((Y_{kji g} - \hat{\mu}_{kji g}) + (\hat{\mu}_{kji g} - \hat{\mu}_{kj g}) + (\hat{\mu}_{kj g} - \hat{\mu}_g))^2, \\
&= \underbrace{\frac{1}{N-1} \sum_{k=1}^K \sum_{j=1}^{n_k} \sum_{i=1}^{n_{kj}} (Y_{kji g} - \hat{\mu}_{kji g})^2}_{\hat{\sigma}_{g1}^2} + \underbrace{\frac{1}{N-1} \sum_{k=1}^K \sum_{j=1}^{n_k} n_{kj} (\hat{\mu}_{kji g} - \hat{\mu}_{kj g})^2}_{\hat{\sigma}_{g2}^2} + \underbrace{\frac{1}{N-1} \sum_{k=1}^K (\sum_{j=1}^{n_k} n_{kj}) \cdot (\hat{\mu}_{kj g} - \hat{\mu}_g)^2}_{\hat{\sigma}_{g3}^2},
\end{aligned}$$

where

$$\hat{\mu}_{kji g} = \frac{1}{n_{kj}} \sum_{i=1}^{n_{kj}} Y_{kji g}, \quad \text{and} \quad \hat{\mu}_{kj g} = \frac{1}{\sum_{j=1}^{n_k} n_{kj}} \sum_{j=1}^{n_k} \sum_{i=1}^{n_{kj}} Y_{kji g}.$$

We remove the variance due to batch effects by redefining $\hat{\sigma}_g^2$ as

$$\hat{\sigma}_g^2 := \hat{\sigma}_{g1}^2 + \hat{\sigma}_{g3}^2,$$

and plug in the redefined variances to the previously described HVG selection procedure.

1.2.2 Seurat style

Pegasus also implements the same HVG selection procedure that Seurat [14] and SCANPY [17] use.

HVG selection in original expression space. In this procedure, we first estimate mean, variance and index of dispersion of each gene g in the original expression space (y_{ig}):

$$\begin{aligned}
\hat{\mu}_g &= \frac{1}{N} \sum_{i=1}^N y_{ig}, \\
\hat{\sigma}_g^2 &= \frac{1}{N-1} \sum_{i=1}^N (y_{ig} - \mu_g)^2, \\
\hat{D}_g &= \frac{\hat{\sigma}_g^2}{\hat{\mu}_g}.
\end{aligned}$$

We then transform the mean and index of dispersion into the log space:

$$\begin{aligned}
\hat{\mu}'_g &= \log(\hat{\mu}_g + 1), \\
\hat{D}'_g &= \log \hat{D}_g.
\end{aligned}$$

In the next step, We group genes into 20 bins based on their mean gene expression levels in the log space $\hat{\mu}'_g$ and calculates z-scores z_g on log index of dispersion within each bin. Let us denote the set of genes in bin j as S_j , we have

$$\begin{aligned}
z_g &= \frac{\hat{D}'_g - \mu_j}{\sigma_j}, \\
\mu_j &= \frac{\sum_{g \in S_j} \hat{D}'_g}{|S_j|}, \\
\sigma_j &= \sqrt{\frac{1}{|S_j| - 1} \sum_{g \in S_j} (\hat{D}'_g - \mu_j)^2}.
\end{aligned}$$

Now we can select HVGs based on the z-scores. Pegasus offers two ways to select HVGs: 1) Select top n genes with largest z-scores, where $n = 2000$ by default; 2) Select all genes satisfying $a < \hat{\mu}'_g < b$ and $c < z_g < d$, where by default $a = 0.0125, b = 7, c = 0.5, d = \infty$. Note that in 2), all defaults are identical to SCANPY except b , where SCANPY's default is $b = 3$.

Handle batch effects. We adopt the method proposed in Seurat V3 [15] to handle batch effects during the HVG selection process. We first select top n HVGs using the previous procedure independently for each batch. We then pool selected HVGs together and rank them by 1) number of batches the gene is in HVG set (descending order), and 2) the median rank in batches where the gene is HVG (ascending order). Lastly, we select the top n genes from the pooled HVGs using the new ranking.

1.3 Batch correction

Pegasus implements the simple location and scale (L/S) adjustment method [8, 10] for batch correction. Because the batch sizes in single-cell RNA-Seq data are very large in general (at least thousands of cells for droplet-based methods), there is no need to stabilize mean and variance estimates by using empirical Bayesian methods, such as the method used in ComBat [8]. We describe our correction method using mathematical notations that are similar to [8].

L/S method. We first consider the scenario that we only have one biological group. Suppose we have m batches and each batch j has n_j cells. We correct batch effects for all G genes and we have N cells, where $N = \sum_{j=1}^m n_j$. We model the log expression of gene g in the i th cell of batch j as

$$Y_{jig} = \alpha_g + \gamma_{jg} + \delta_{jg}\epsilon_{jig}, \quad \epsilon_{jig} \sim \text{Dist}(0, \sigma_g^2),$$

where α_g is the average expression of gene g , and ϵ_{jig} is the error term following a distribution with 0 mean and σ_g^2 variance. γ_{jg} and δ_{jg} are the additive and multiplicative batch effects for gene g in batch j respectively. In the L/S method, we adjust the batch effects for each gene separately.

Parameter estimation. Let $\ddot{\gamma}_{jg} = \alpha_g + \gamma_{jg}$, we have $Y_{jig} = \ddot{\gamma}_{jg} + \delta_{jg}\epsilon_{jig}$. The mean square error (MSE) estimate of $\ddot{\gamma}_{jg}$ is

$$\widehat{\ddot{\gamma}}_{jg} = \hat{\alpha}_g + \hat{\gamma}_{jg} = \frac{1}{n_j} \sum_{i=1}^{n_j} Y_{jig}.$$

To make sure the model is identifiable, we further impose the constraint that $\sum_j n_j \hat{\gamma}_{jg} = 0$ [8]. With this constraint, we estimate α_g and γ_{jg} as

$$\begin{aligned} \hat{\alpha}_g &= \frac{1}{N} \sum_{j=1}^m \sum_{i=1}^{n_j} Y_{jig}, \\ \hat{\gamma}_{jg} &= \frac{1}{n_j} \sum_{i=1}^{n_j} Y_{jig} - \hat{\alpha}_g. \end{aligned}$$

Following [8], we estimate σ_g as

$$\hat{\sigma}_g = \sqrt{\frac{1}{N} \sum_{j=1}^m \sum_{i=1}^{n_j} (Y_{jig} - \hat{\alpha}_g - \hat{\gamma}_{jg})^2}.$$

Lastly, δ_{jg} can be estimated as

$$\hat{\delta}_{jg} = \frac{\sqrt{\frac{1}{n_j-1} \sum_{i=1}^{n_j} (Y_{jig} - \hat{\alpha}_g - \hat{\gamma}_{jg})^2}}{\hat{\sigma}_g}.$$

Adjust batch effects. Let us denote the adjusted expression level as Y_{jig}^* , we have:

$$Y_{jig}^* = \frac{Y_{jig} - \hat{\alpha}_g - \hat{\gamma}_{jg}}{\hat{\delta}_{jg}} + \hat{\alpha}_g.$$

Multiple biological groups. Suppose we have K groups of biological samples, each group k has n_k batches and each batch kj has n_{kj} cells. We further assume that any differences between the K groups are biological. We model the log gene expression level as

$$Y_{kjig} = \alpha_{kg} + \gamma_{kjg} + \delta_{kjg}\epsilon_{kjig}, \quad \epsilon_{kjig} \sim \text{Dist}(0, \sigma_{kg}^2),$$

adjust batch effects as

$$Y_{kjig}^* = \frac{Y_{kjig} - \hat{\alpha}_{kg} - \hat{\gamma}_{kjg}}{\hat{\delta}_{kjg}} + \hat{\alpha}_{kg}.$$

1.4 Diffusion map and diffusion-based pseudotime

Pegasus implements the diffusion pseudotime (DPT) algorithm proposed in [6] with several improvements. To speed up the calculation of diffusion maps, we adopt 2 tricks that SCANPY [17] also uses: 1) constructing affinity matrix based on approximated kNN graph instead of the complete graph; 2) using only the top n diffusion components to approximate diffusion distances, where n is a user-specified parameter. In addition, based on diffusion maps, we define a family of diffusion pseudotime maps parameterized by timescale t , where the DPT algorithm corresponds to a diffusion pseudotime map with $t = \infty$. We provide a principled way of picking t so that the corresponding diffusion pseudotime map reveals the embedded developmental trajectory better.

In the following, we first summarize how we compute diffusion maps. We then introduce how to calculate diffusion pseudotime maps and choose appropriate timescale t . Lastly, we describe how to approximate diffusion pseudotime maps with top n components and how to calculate diffusion-based pseudotimes.

1.4.1 Affinity matrix construction

Following [6], we put an isotropic Gaussian wave function on each cell \mathbf{x} , where $\mathbf{x} = (x_1, \dots, x_n)^T$ represents the coordinates of this cell on top n principal components:

$$Y_{\mathbf{x}}(\mathbf{x}') = \left(\frac{2}{\pi\sigma_{\mathbf{x}}^2} \right)^{\frac{1}{4}} \exp \left(-\frac{\|\mathbf{x}' - \mathbf{x}\|^2}{\sigma_{\mathbf{x}}^2} \right).$$

The kernel width $\sigma_{\mathbf{x}}$ is adjusted according to each cell \mathbf{x} . Suppose d_1, \dots, d_K are the distances between cell \mathbf{x} and its K nearest neighbors. Since \mathbf{x} 's 1st nearest neighbor is itself, $d_1 = 0$. We estimate $\sigma_{\mathbf{x}}$ as

$$\sigma_{\mathbf{x}} = \text{median} \{d_i \mid i = 2, \dots, K\}.$$

The interference of the wave functions of two cells \mathbf{x} and \mathbf{y} results in a locally-scaled Gaussian kernel [5, 18]:

$$\begin{aligned}
K(\mathbf{x}, \mathbf{y}) &= \int_{-\infty}^{\infty} Y_{\mathbf{x}}(\mathbf{x}') Y_{\mathbf{y}}(\mathbf{x}') d\mathbf{x}' \\
&= \int_{-\infty}^{\infty} \left(\frac{2}{\pi \sigma_{\mathbf{x}}^2} \right)^{\frac{1}{4}} \exp \left(-\frac{\|\mathbf{x}' - \mathbf{x}\|^2}{\sigma_{\mathbf{x}}^2} \right) \cdot \left(\frac{2}{\pi \sigma_{\mathbf{y}}^2} \right)^{\frac{1}{4}} \exp \left(-\frac{\|\mathbf{x}' - \mathbf{y}\|^2}{\sigma_{\mathbf{y}}^2} \right) d\mathbf{x}' \\
&= \int_{-\infty}^{\infty} \left(\frac{2}{\pi \sigma_{\mathbf{x}} \sigma_{\mathbf{y}}} \right)^{\frac{1}{2}} \exp \left(-\frac{\sigma_{\mathbf{y}}^2 (\mathbf{x}' - \mathbf{x})^T (\mathbf{x}' - \mathbf{x}) + \sigma_{\mathbf{x}}^2 (\mathbf{x}' - \mathbf{y})^T (\mathbf{x}' - \mathbf{y})}{\sigma_{\mathbf{x}}^2 \sigma_{\mathbf{y}}^2} \right) d\mathbf{x}' \\
&= \int_{-\infty}^{\infty} \left(\frac{2}{\pi \sigma_{\mathbf{x}} \sigma_{\mathbf{y}}} \right)^{\frac{1}{2}} \exp \left(-\frac{\sigma_{\mathbf{x}}^2 + \sigma_{\mathbf{y}}^2}{\sigma_{\mathbf{x}}^2 \sigma_{\mathbf{y}}^2} \left[\mathbf{x}'^T \mathbf{x}' - 2 \left(\frac{\sigma_{\mathbf{y}}^2 \mathbf{x} + \sigma_{\mathbf{x}}^2 \mathbf{y}}{\sigma_{\mathbf{x}}^2 + \sigma_{\mathbf{y}}^2} \right)^T \mathbf{x}' + \left(\frac{\sigma_{\mathbf{y}}^2 \mathbf{x} + \sigma_{\mathbf{x}}^2 \mathbf{y}}{\sigma_{\mathbf{x}}^2 + \sigma_{\mathbf{y}}^2} \right)^T \left(\frac{\sigma_{\mathbf{y}}^2 \mathbf{x} + \sigma_{\mathbf{x}}^2 \mathbf{y}}{\sigma_{\mathbf{x}}^2 + \sigma_{\mathbf{y}}^2} \right) \right] \right) \\
&\quad \cdot \exp \left(-\frac{\mathbf{x}^T \mathbf{x} - 2 \mathbf{x}^T \mathbf{y} + \mathbf{y}^T \mathbf{y}}{\sigma_{\mathbf{x}}^2 + \sigma_{\mathbf{y}}^2} \right) d\mathbf{x}' \\
&= \left(\frac{2 \sigma_{\mathbf{x}} \sigma_{\mathbf{y}}}{\sigma_{\mathbf{x}}^2 + \sigma_{\mathbf{y}}^2} \right)^{\frac{1}{2}} \exp \left(-\frac{\|\mathbf{x} - \mathbf{y}\|^2}{\sigma_{\mathbf{x}}^2 + \sigma_{\mathbf{y}}^2} \right) \cdot \int_{-\infty}^{\infty} \left(\frac{1}{2 \pi \frac{\sigma_{\mathbf{x}}^2 \sigma_{\mathbf{y}}^2}{\sigma_{\mathbf{x}}^2 + \sigma_{\mathbf{y}}^2}} \right)^{\frac{1}{2}} \exp \left(-\frac{\|\mathbf{x}' - \frac{\sigma_{\mathbf{y}}^2 \mathbf{x} + \sigma_{\mathbf{x}}^2 \mathbf{y}}{\sigma_{\mathbf{x}}^2 + \sigma_{\mathbf{y}}^2}\|^2}{2 \frac{\sigma_{\mathbf{x}}^2 \sigma_{\mathbf{y}}^2}{\sigma_{\mathbf{x}}^2 + \sigma_{\mathbf{y}}^2}} \right) d\mathbf{x}' \\
&= \left(\frac{2 \sigma_{\mathbf{x}} \sigma_{\mathbf{y}}}{\sigma_{\mathbf{x}}^2 + \sigma_{\mathbf{y}}^2} \right)^{\frac{1}{2}} \exp \left(-\frac{\|\mathbf{x} - \mathbf{y}\|^2}{\sigma_{\mathbf{x}}^2 + \sigma_{\mathbf{y}}^2} \right).
\end{aligned}$$

To construct the affinity matrix, we find the top K nearest neighbors for each cell ($K = 100$ by default) using the state-of-the-art approximate nearest neighbor finding algorithm HNSW [11]. We then construct a sparse matrix \mathbf{W}_1 using the locally-scaled Gaussian kernel as follows:

$$\mathbf{W}_1(i, j) = \begin{cases} K(\mathbf{x}_i, \mathbf{x}_j), & j \neq i \text{ and } j \text{ is in } i\text{'s } K \text{ nearest neighbors} \\ 0, & \text{otherwise} \end{cases}.$$

Note that we exclude the 1st nearest neighbor of each cell, which is the cell itself, in the above equation.

We then obtain symmetrized matrix \mathbf{W}_2 by symmetrizing \mathbf{W}_1 as follows:

$$\mathbf{W}_2(i, j) = \begin{cases} \mathbf{W}_1(i, j), & \mathbf{W}_1(i, j) > 0 \\ \mathbf{W}_1(j, i), & \mathbf{W}_1(i, j) = 0 \text{ and } \mathbf{W}_1(j, i) > 0 \\ 0, & \text{otherwise} \end{cases}.$$

We assume the transcriptomic landscape is embedded in a low-dimensional manifold. Since there is no guarantee that the manifold is uniformly sampled and the sampling density is not necessarily related to the geometry of the manifold, we need to normalize each cell by its sampling density. Following [4], we first define the sampling density term $q(\mathbf{x}_i)$ for each cell i :

$$q(\mathbf{x}_i) = \sum_{j=1}^N \mathbf{W}_2(i, j).$$

We then define an anisotropic kernel $K'(\mathbf{x}, \mathbf{y})$, which normalize the affinity between \mathbf{x} and \mathbf{y} by their sampling density terms:

$$K'(\mathbf{x}, \mathbf{y}) = \frac{K(\mathbf{x}, \mathbf{y})}{q(\mathbf{x})q(\mathbf{y})}.$$

We have an intuitive way to understand the above normalization. Suppose cell i connects to cell j , which has a high sampling density and to cell k , which has a low sampling density. Then it is likely that i connects to much more cells in j 's local neighborhood than k 's local neighborhood. After dividing the sampling density

terms at j and k , the total contributions of j 's neighborhood and k 's neighborhood to cell i can be roughly equal.

By applying the anisotropic kernel to \mathbf{W}_2 , we obtain the affinity matrix \mathbf{W} , which can recover the Riemannian geometry of the data, regardless of the sampling density [4]:

$$\mathbf{W}_{ij} = \frac{\mathbf{W}_2(i, j)}{q(\mathbf{x}_i)q(\mathbf{x}_j)}.$$

1.4.2 Markov chain transition probability matrix

We define the Markov chain transition probability matrix \mathbf{P} based on the affinity matrix \mathbf{W} :

$$\mathbf{P} = \mathbf{D}^{-1}\mathbf{W}, \quad \text{where } \mathbf{D} = \text{diag}\left(\sum_{j=1}^N \mathbf{W}_{ij}\right) \text{ is the degree matrix.}$$

The transition matrix \mathbf{P} is not symmetric. We define the symmetric normalized transition matrix \mathbf{Q} as

$$\mathbf{Q} = \mathbf{D}^{-\frac{1}{2}}\mathbf{W}\mathbf{D}^{-\frac{1}{2}},$$

and we have

$$\mathbf{P} = \mathbf{D}^{-\frac{1}{2}}\mathbf{Q}\mathbf{D}^{\frac{1}{2}}.$$

Since \mathbf{Q} is real symmetric, it has the following eigen decomposition:

$$\mathbf{Q} = \mathbf{U}\mathbf{\Lambda}\mathbf{U}^T.$$

Lemma 1. \mathbf{Q} 's eigenvalues λ_i s are bounded between $[-1, 1]$.

Proof. We define $\mathbf{L}^{sym} = \mathbf{I} - \mathbf{Q}$, which is the symmetric normalized Laplacian matrix. \mathbf{L}^{sym} is positive semidefinite because for any vector \mathbf{c} , we have

$$\frac{\mathbf{c}^T \mathbf{L}^{sym} \mathbf{c}}{\mathbf{c}^T \mathbf{c}} = \frac{\mathbf{c}^T (\mathbf{I} - \mathbf{Q}) \mathbf{c}}{\mathbf{c}^T \mathbf{c}} = \frac{\sum_{i,j:i < j, \mathbf{Q}_{ij} > 0} K'(\mathbf{x}_i, \mathbf{x}_j) \left(\frac{c_i}{\sqrt{d_i}} - \frac{c_j}{\sqrt{d_j}} \right)^2}{\|\mathbf{c}\|^2} \geq 0.$$

We denote \mathbf{L}^{sym} 's eigenvalues as λ'_i s. We know \mathbf{L}^{sym} and \mathbf{Q} share the same eigenvectors and $\lambda_i = 1 - \lambda'_i$.

$$\begin{aligned} \mathbf{L}^{sym} \mathbf{u}_i &= \lambda'_i \mathbf{u}_i \\ \Leftrightarrow (\mathbf{I} - \mathbf{Q}) \mathbf{u}_i &= \lambda'_i \mathbf{u}_i \\ \Leftrightarrow \mathbf{Q} \mathbf{u}_i &= (1 - \lambda'_i) \mathbf{u}_i \\ \Leftrightarrow \mathbf{Q} \mathbf{u}_i &= \lambda_i \mathbf{u}_i. \end{aligned}$$

Since $\lambda'_i \geq 0$, we have $\lambda_i = 1 - \lambda'_i \leq 1$.

In addition, we can show $\lambda = 1$ and $\mathbf{u} = \mathbf{D}^{\frac{1}{2}} \mathbf{1}$ is an eigenvalue for \mathbf{Q} :

$$\mathbf{Q} \mathbf{u} = \mathbf{D}^{-\frac{1}{2}} \mathbf{W} \mathbf{D}^{-\frac{1}{2}} \cdot \mathbf{D}^{\frac{1}{2}} \mathbf{1} = \mathbf{D}^{-\frac{1}{2}} \cdot \mathbf{W} \mathbf{1} = \mathbf{D}^{-\frac{1}{2}} \mathbf{D} \cdot \mathbf{1} = \mathbf{D}^{\frac{1}{2}} \mathbf{1} = \mathbf{u}.$$

Similarly, we can show that $\mathbf{I} + \mathbf{Q}$ is also positive semidefinite since for any vector \mathbf{c} , we have

$$\frac{\mathbf{c}^T(\mathbf{I} + \mathbf{Q})\mathbf{c}}{\mathbf{c}^T\mathbf{c}} = \frac{\sum_{i,j:i < j, \mathbf{Q}_{ij} > 0} K'(\mathbf{x}_i, \mathbf{x}_j) \left(\frac{c_i}{\sqrt{d_i}} + \frac{c_j}{\sqrt{d_j}} \right)^2}{\|\mathbf{c}\|^2} \geq 0.$$

Thus, $1 + \lambda_i \geq 0 \Rightarrow \lambda_i \geq -1$.

Note that $\lambda_i = -1$ only if one of the connected component is a bipartite graph.

□

In practice, our single cell data always result in a connected graph. Thus, we assume eigenvalue $\lambda = 1$ only has one eigenvector. In addition, since we always observe cliques of at least 3 cells, it is unlikely the connected graph is a bipartite graph. Thus, we also assume that $\lambda_i > -1$.

We order \mathbf{Q} 's eigenvalues by their magnitudes: $1 = \lambda_0 > |\lambda_1| \geq |\lambda_2| \geq \dots \geq |\lambda_{N-1}|$.

Now we can find \mathbf{P} 's eigen decomposition via \mathbf{Q} 's. We have

$$\begin{aligned} \mathbf{P} &= \mathbf{D}^{-\frac{1}{2}} \mathbf{Q} \mathbf{D}^{\frac{1}{2}} \\ &= \mathbf{D}^{-\frac{1}{2}} \cdot \mathbf{U} \mathbf{\Lambda} \mathbf{U}^T \cdot \mathbf{D}^{\frac{1}{2}} \\ &= (\mathbf{D}^{-\frac{1}{2}} \mathbf{U}) \mathbf{\Lambda} (\mathbf{D}^{\frac{1}{2}} \mathbf{U})^T \\ &= \mathbf{\Psi} \mathbf{\Lambda} \mathbf{\Phi}^T, \end{aligned}$$

where $\mathbf{\Psi} = \mathbf{D}^{-\frac{1}{2}} \mathbf{U}$ are \mathbf{P} 's right eigenvectors and $\mathbf{\Phi} = \mathbf{D}^{\frac{1}{2}} \mathbf{U}$ are \mathbf{P} 's left eigenvectors. In addition, we have

$$\mathbf{\Phi}^T \mathbf{\Psi} = \mathbf{U}^T \mathbf{D}^{\frac{1}{2}} \cdot \mathbf{D}^{-\frac{1}{2}} \mathbf{U} = \mathbf{U}^T \mathbf{U} = \mathbf{I}.$$

Note that the right eigenvector of $\lambda_0 = 1$ for \mathbf{P} becomes

$$\psi_0 = \mathbf{D}^{-\frac{1}{2}} \mathbf{u}_0 = \mathbf{D}^{-\frac{1}{2}} \cdot \mathbf{D}^{\frac{1}{2}} \mathbf{1} = \mathbf{1}.$$

1.4.3 Diffusion maps and diffusion distances

We define a family of diffusion maps $\{\mathbf{\Psi}_t\}_{t \in \mathbb{N}}$ as

$$\mathbf{\Psi}_t(\mathbf{x}_i) = \begin{pmatrix} \lambda_1^t \psi_1(i) \\ \lambda_2^t \psi_2(i) \\ \vdots \\ \lambda_{N-1}^t \psi_{N-1}(i) \end{pmatrix},$$

and associated diffusion distances as

$$D_t(\mathbf{x}_i, \mathbf{x}_j) = \|\mathbf{\Psi}_t(\mathbf{x}_i) - \mathbf{\Psi}_t(\mathbf{x}_j)\| = \left(\sum_{l=1}^{N-1} \lambda_l^{2t} (\psi_l(i) - \psi_l(j))^2 \right)^{\frac{1}{2}}.$$

In above definitions, we omit diffusion component 0, Ψ_0 , since all its components are the same and thus have no influence on the distance.

We can show that the diffusion distance D_t is equal to the weighted ℓ^2 distance between transition probabilities after t steps.

Let us define $p_t(\cdot, \cdot)$ as the transition probabilities between any two cells after t steps:

$$\begin{aligned}
p_t(\cdot, \cdot) &= \mathbf{P}^t \\
&= \mathbf{\Psi} \mathbf{\Lambda} \mathbf{\Phi}^T \cdot \mathbf{\Psi} \mathbf{\Lambda} \mathbf{\Phi}^T \dots \mathbf{\Psi} \mathbf{\Lambda} \mathbf{\Phi}^T \\
&= \mathbf{\Psi} \mathbf{\Lambda}^t \mathbf{\Phi} \\
&= \sum_{l=0}^{N-1} \lambda_l^t \psi_l \phi_l^T.
\end{aligned}$$

Lemma 2.

$$D_t(\mathbf{x}_i, \mathbf{x}_j) = \|p_t(\mathbf{x}_i, \cdot) - p_t(\mathbf{x}_j, \cdot)\|_{\ell^2(\mathbb{R}^N, \frac{1}{d})}$$

Proof.

$$\begin{aligned}
\|p_t(\mathbf{x}_i, \cdot) - p_t(\mathbf{x}_j, \cdot)\|_{\ell^2(\mathbb{R}^N, \frac{1}{d})}^2 &= \sum_{k=1}^N (\mathbf{P}_{ik}^t - \mathbf{P}_{jk}^t)^2 \cdot \frac{1}{d_k} \\
&= \sum_{k=1}^N \left(\sum_{l=0}^{N-1} \lambda_l^t \psi_l(i) \phi_l(k) - \sum_{l=0}^{N-1} \lambda_l^t \psi_l(j) \phi_l(k) \right)^2 \cdot \frac{1}{d_k} \\
&= \sum_{k=1}^N \left(\sum_{l=0}^{N-1} \lambda_l^t (\psi_l(i) - \psi_l(j)) \phi_l(k) \right)^2 \cdot \frac{1}{d_k} \\
&= \sum_{k=1}^N \sum_{l=0}^{N-1} \sum_{l'=0}^{N-1} \lambda_l^t \lambda_{l'}^t (\psi_l(i) - \psi_l(j)) (\psi_{l'}(i) - \psi_{l'}(j)) \frac{\phi_l(k) \phi_{l'}(k)}{d_k} \\
&= \sum_{l=0}^{N-1} \sum_{l'=0}^{N-1} \lambda_l^t \lambda_{l'}^t (\psi_l(i) - \psi_l(j)) (\psi_{l'}(i) - \psi_{l'}(j)) \frac{\sum_{k=1}^N \phi_l(k) \phi_{l'}(k)}{d_k} \\
&= \sum_{l=0}^{N-1} \lambda_l^{2t} (\psi_l(i) - \psi_l(j))^2 \\
&= \sum_{l=1}^{N-1} \lambda_l^{2t} (\psi_l(i) - \psi_l(j))^2 \\
&= D_t(\mathbf{x}_i, \mathbf{x}_j)^2.
\end{aligned}$$

□

A diffusion map $\mathbf{\Psi}_t$ with small t reveals local geometric properties and is less robust to noise. In contrast, $\mathbf{\Psi}_t$ with large t reveals global geometric properties and is more robust.

1.4.4 Diffusion pseudotime maps

We define a family of diffusion pseudotime maps $\{\mathbf{\Psi}'_t\}_{t \in \mathbb{N}}$ as

$$\begin{aligned}
\mathbf{\Psi}'_t(\mathbf{x}_i) &= \sum_{t'=1}^t \mathbf{\Psi}_{t'}(\mathbf{x}_i) \\
&= \begin{pmatrix} \sum_{t'=1}^t \lambda_1^{t'} \psi_1(i) \\ \sum_{t'=1}^t \lambda_2^{t'} \psi_2(i) \\ \vdots \\ \sum_{t'=1}^t \lambda_{N-1}^{t'} \psi_{N-1}(i) \end{pmatrix} \\
&= \begin{pmatrix} \lambda_1 \frac{1-\lambda_1^t}{1-\lambda_1} \psi_1(i) \\ \lambda_2 \frac{1-\lambda_2^t}{1-\lambda_2} \psi_2(i) \\ \vdots \\ \lambda_{N-1} \frac{1-\lambda_{N-1}^t}{1-\lambda_{N-1}} \psi_{N-1}(i) \end{pmatrix}.
\end{aligned}$$

The associated diffusion pseudotime distances are

$$D'_t(\mathbf{x}_i, \mathbf{x}_j) = \|\Psi'_t(\mathbf{x}_i) - \Psi'_t(\mathbf{x}_j)\| = \left(\sum_{l=1}^{N-1} \left[\lambda_l \frac{1 - \lambda_l^t}{1 - \lambda_l} \cdot (\psi_l(i) - \psi_l(j))^2 \right] \right)^{\frac{1}{2}}.$$

If we set $t = \infty$, we recover the DPT algorithm [6], which sums diffusion maps over all timescales. However, when the timescale t becomes large enough, the corresponding diffusion map begins to smooth out real signals [12, 16]. In the extreme case $t = \infty$, all signals are smoothed out and the diffusion distance between any pair of cells is 0. Thus, $t = \infty$ might lose important biological signals. In Pegasus, we seek to pick a t that smooth out most noise but little signal.

von Neumann Entropy. Inspired by the PHATE [12] work, we choose t based on the von Neumann entropy [1] of the graph induced by each timescale. For each timescale t , the power matrix \mathbf{P}^t induces a graph. Since \mathbf{P}^t is a transition matrix, its degree matrix \mathbf{D} is always equal to the identity matrix \mathbf{I} , and its Laplacian matrix becomes

$$\begin{aligned} \mathbf{L}(t) &= \mathbf{I} - \mathbf{P}^t \\ &= \mathbf{\Psi} \mathbf{\Phi}^T - \mathbf{\Psi} \mathbf{\Lambda}^t \mathbf{\Phi}^T \\ &= \mathbf{\Psi} (\mathbf{I} - \mathbf{\Lambda}^t) \mathbf{\Phi}^T. \end{aligned}$$

Thus $\mathbf{L}(t)$ shares the same eigenvectors as \mathbf{P} and have eigenvalues $1 - \lambda_0^t, \dots, 1 - \lambda_{N-1}^t$.

We then derive \mathbf{P}^t 's graph density matrix $\rho(\mathbf{L}(t))$ by normalizing $\mathbf{L}(t)$'s trace to 1:

$$\rho(\mathbf{L}(t)) = \frac{\mathbf{L}(t)}{\text{tr}(\mathbf{L}(t))}, \quad \text{where } \text{tr}(\mathbf{L}(t)) = \sum_{i=0}^{N-1} 1 - \lambda_i^t.$$

Let us denote the density matrix's eigenvalues as $[\eta(t)]_0, \dots, [\eta(t)]_{N-1}$, we have

$$[\eta(t)]_i = \frac{1 - \lambda_i^t}{\sum_{j=0}^{N-1} 1 - \lambda_j^t} \quad \text{and} \quad \sum_{i=0}^{N-1} [\eta(t)]_i = 1.$$

The von Neumann entropy $S(t)$ is defined on the density matrix $\rho(\mathbf{L}_t)$:

$$\begin{aligned} S(t) &= -\text{tr}(\rho(\mathbf{L}(t)) \log \rho(\mathbf{L}(t))) \\ &= -\sum_{i=0}^{N-1} [\eta(t)]_i \log [\eta(t)]_i. \end{aligned}$$

$S(t)$ increases as t increases and reaches its maximum $S(t) = \log(N - 1)$ when $t \rightarrow \infty$. As t increases, the smaller eigenvalues (likely representing noise) of transition matrix \mathbf{P} decreases to 0 (and eigenvalue of 1 for $\mathbf{L}(t)$) much more rapidly than the larger eigenvalues (likely representing signals) [12]. Thus, we can observe a high rate of increase in $S(t)$ initially when data noise is reduced and then a low rate of increase in $S(t)$ when signal is smoothed out.

If we plot $S(t)$ against t , we can see a knee-shaped curve and we pick the best t as the knee point of this curve.

Picking knee point. To find the knee point, we consider all ts in the range of $[1, \text{maxt}]$, where maxt is a user-specified parameter (default: $\text{maxt} = 5000$). We draw a segment between $t = 1$ and $t = \text{maxt}$ and find the point in curve that is furthest from the segment by scanning $t = 2, \dots, \text{maxt} - 1$.

We define $p_1 = \begin{bmatrix} 1 \\ S(1) \end{bmatrix}$ and $p_2 = \begin{bmatrix} \text{maxt} \\ S(\text{maxt}) \end{bmatrix}$ as the two end points, and let $p_3 = \begin{bmatrix} t \\ S(t) \end{bmatrix}$ as the point we scan.

We can calculate the distance between p_3 and segment $p_2 - p_1$ as

$$dis = \frac{\|(p_3 - p_1) \times (p_2 - p_1)\|}{\|p_2 - p_1\|}.$$

1.4.5 Approximation

Diffusion components with eigenvalues close to 0 contribute little to the diffusion distance. This implies that we can approximate the distance by only keeping the top n diffusion components. Since we exclude diffusion component 0 (Ψ_0), we keep $n - 1$ diffusion components in practice. Pegasus uses $n = 100$ by default.

Compute top n eigenvalues and eigenvectors. We use the Implicitly Restarted Lanczos Method [2] (via `scipy.sparse.linalg.eigsh` function) to calculate the top n eigenvalues and eigenvectors of \mathbf{Q} .

We also provide an option to compute top n eigenvalues and eigenvectors using the randomized SVD algorithm [7] implemented in scikit-learn [13] as follows:

Suppose \mathbf{Q} 's SVD decomposition is as follows:

$$\mathbf{Q} \approx \mathbf{U}_{N \times n} \cdot \mathbf{S}_{n \times n} \cdot \mathbf{V}_{n \times N}^T.$$

We know that $\mathbf{U}_{N \times n}$ are the top n eigenvectors of \mathbf{Q} . However, the singular values are not necessarily equal to the eigenvalues. In particular, we have

$$\sigma_i = \sqrt{\lambda_i^2} = |\lambda_i|,$$

which means the singular values lose the signs.

We use $\mathbf{V}_{n \times N}^T$ to help us recover the signs. We know that

$$\mathbf{v}_i = \frac{\mathbf{Q}^T \mathbf{u}_i}{\sigma_i} = \frac{\lambda_i \mathbf{u}_i}{\sigma_i} = \text{sign}(\lambda_i) \mathbf{u}_i,$$

and thus

$$\mathbf{V}_{n \times N}^T \cdot \mathbf{U}_{N \times n} = \begin{pmatrix} \text{sign}(\lambda_0) & 0 & \cdots & 0 \\ 0 & \text{sign}(\lambda_1) & \cdots & 0 \\ \vdots & \vdots & \ddots & \vdots \\ 0 & 0 & \cdots & \text{sign}(\lambda_{n-1}) \end{pmatrix}.$$

Therefore, we can calculate eigenvalues $\mathbf{\Lambda}_{n \times n}$ as

$$\mathbf{\Lambda}_{n \times n} = (\mathbf{V}_{n \times N}^T \mathbf{U}_{N \times n}) \cdot \mathbf{S}_{n \times n}.$$

von Neumann entropy for top n eigenvalues. If we only focus on the top n eigenvalues, we obtain the following truncated Laplacian matrix:

$$\tilde{\mathbf{L}}(t) = \sum_{i=0}^{n-1} (1 - \lambda_i^t) \psi_i \phi_i^T,$$

and its density matrix:

$$\rho(\tilde{\mathbf{L}}(t)) = \frac{\tilde{\mathbf{L}}(t)}{\text{tr}(\tilde{\mathbf{L}}(t))}, \quad \text{where } \text{tr}(\tilde{\mathbf{L}}(t)) = \sum_{i=0}^{n-1} 1 - \lambda_i^t.$$

Thus, the von Neumann entropy becomes

$$S(t) := - \sum_{i=0}^{n-1} [\eta'(t)]_i \log[\eta'(t)]_i, \quad \text{where } [\eta'(t)]_i = \frac{1 - \lambda_i^t}{\sum_{j=0}^{n-1} 1 - \lambda_j^t}.$$

1.4.6 Diffusion-based pseudotime calculation

Suppose users select a set of m cells as roots, we first calculate the diffusion-based distance for each cell as follows:

$$dis(\mathbf{x}_i, roots) = \frac{1}{m} \sum_{j \in roots} D'_t(\mathbf{x}_i, \mathbf{x}_j) \approx \frac{1}{m} \sum_{j \in roots} \left(\sum_{l=1}^{n-1} \left[\lambda_l \frac{1 - \lambda_l^t}{1 - \lambda_l} \cdot (\psi_l(i) - \psi_l(j)) \right]^2 \right)^{\frac{1}{2}}.$$

Then we normalize these distances to between $[0, 1]$ to obtain our diffusion-based pseudotimes:

$$pseudotime(\mathbf{x}_i) = \frac{dis(\mathbf{x}_i, roots) - \min_j dis(\mathbf{x}_j, roots)}{\max_j dis(\mathbf{x}_j, roots) - \min_j dis(\mathbf{x}_j, roots)}.$$

2 Supplementary Note 2

2.1 Function calls, commands and parameters used for benchmarking Pegasus, SCANPY and Seurat on the full bone marrow dataset (Supplementary Table 4)

Seurat. We first set `plan("multiprocess", workers=28)`. Next, we ran `SelectIntegrationFeatures` with parameters `mean.cutoff=c(0.0125, 7)` and `dispersion.cutoff=c(0.5, Inf)` for HVG selection; corrected batch effects for all 63 10x channels by calling `FindIntegrationAnchors` and `IntegrateData` with default parameters; ran `ScaleData` with default parameters and `RunPCA` with `seed.use=0` for PCA computation; ran `FindNeighbors` with `k.param=100`, `compute.SNN=FALSE`, `dims=1:50` and `nn.method="annoy"` to find k neighbors; ran `FindClusters` with `resolution=1.3`, `random.seed=0` and `algorithm="louvain"` or `algorithm="leiden"` to find clusters using either Louvain or Leiden algorithm; ran `RunTSNE` with `seed.use=0`, `dims=1:50` and `tsne.method="FIt-SNE"` to calculate tSNE-like visualization; ran `RunUMAP` with `seed.use=0`, `umap.method="umap-learn"`, `metric="correlation"`, `n.neighbors=15`, `min.dist=0.5` and `dims=1:50` to calculate UMAP-like visualization.

SCANPY. We first set `scanpy.settings.n_jobs=28`. Next, we ran `scanpy.pp.highly_variable_genes` with parameters `min_mean=0.0125`, `max_mean=7`, `min_disp=0.5`, `n_top_genes=2000` and `batch_key='Channel'` for HVG selection; imported `bbknn` python package directly and ran `bbknn.bbknn` with parameter `batch_key = 'Channel'` to correct batch effects; ran `scanpy.pp.scale` with parameter `max_value=10` and then `scanpy.tl.pca` with parameter `random_state=0` to compute PCA; ran `scanpy.pp.neighbors` with parameters `n_neighbors=100` and `random_state=0` to find k neighbors; ran `scanpy.tl.diffmap` with parameter `n_comps=100` to compute diffusion map; ran `scanpy.tl.louvain` and `scanpy.tl.leiden` with parameters `resolution=1.3` and `random_state=0` for Louvain and Leiden clusterings; ran `scanpy.tl.tsne` with parameters `use_rep='X_pca'`, `random_state=0` and `use_fast_tsne=True` to compute t-SNE; ran `scanpy.tl.umap` with parameter `random_state=0` to compute UMAP; ran `scanpy.tl.draw_graph` with parameters `random_state=0` and `iterations=500` to compute FLE.

Pegasus. We ran `pegasus cluster` with parameters `-p 28 --correct-batch-effect --knn-full-speed --diffmap --spectral-louvain --spectral-leiden --fitsne --net-umap --net-file`.

2.2 Function calls, commands and parameters used for benchmarking Pegasus, SCANPY and Seurat v3 on the 1.3 million mouse brain dataset (Supplementary Table 5)

Seurat. Seurat failed to load this big dataset into memory.

SCANPY. SCANPY function calls and parameters were set exactly the same as in the bone marrow benchmarking experiment.

Pegasus. We ran `pegasus cluster` with parameters `-p 28 --correct-batch-effect --knn-full-speed --diffmap --spectral-louvain --spectral-leiden --fitsne --net-umap --net-file --file-memory 128`.

2.3 Commands for benchmarking Pegasus components on subsampled bone marrow datasets (Supplementary Data 2)

We ran `pegasus cluster` with parameters `-p n_cpu --correct-batch-effect --knn-full-speed --diffmap --louvain --spectral-louvain --leiden --spectral-leiden --fitsne --tsne --umap --net-umap --file --net-file` on each of the 7 datasets. `n_cpu` was set to 28 for the cloud setting and to 8 for the laptop setting.

2.4 Function calls, commands and parameters used for benchmarking Pegasus, SCANPY and Seurat on the 5K PBMC dataset using 8 threads (Supplementary Table 6)

Seurat. We first set `plan("multiprocess", workers=8)`. Next, we ran `FindVariableFeatures` with parameters `mean.cutoff=c(0.0125, 7)` and `dispersion.cutoff=c(0.5, Inf)` for HVG selection; ran `ScaleData` with default parameters and `RunPCA` with `seed.use=0` for PCA computation; ran `FindNeighbors` with `k.param=100`, `compute.SNN=FALSE`, `dims=1:50` and `nn.method="annoy"` to find k neighbors; ran `FindClusters` with `resolution=1.3`, `random.seed=0` and `algorithm="louvain"` or `algorithm="leiden"` to find clusters using either Louvain or Leiden algorithm; ran `RunTSNE` with `seed.use=0`, `dims=1:50` and `tsne.method="FIt-SNE"` to calculate tSNE-like visualization; ran `RunUMAP` with `seed.use=0`, `umap.method="umap-learn"`,

`metric="correlation", n.neighbors=15, min.dist=0.5 and dims=1:50` to calculate UMAP-like visualization.

SCANPY. We first set `scanpy.settings.n_jobs=8`. Next, we ran `scanpy.pp.highly_variable_genes` with parameters `min_mean=0.0125, max_mean=7, min_disp=0.5` and `n_top_genes=2000` for HVG selection; ran `scanpy.pp.scale` with parameter `max_value=10` and then `scanpy.tl.pca` with parameter `random_state=0` to compute PCA; ran `scanpy.pp.neighbors` with parameters `n_neighbors=100` and `random_state=0` to find k neighbors; ran `scanpy.tl.diffmap` with parameter `n_comps=100` to compute diffusion map; ran `scanpy.tl.louvain` and `scanpy.tl.leiden` with parameters `resolution=1.3` and `random_state=0` for Louvain and Leiden clusterings; ran `scanpy.tl.tsne` with parameters `use_rep='X_pca', random_state=0` and `use_fast_tsne=True` to compute t-SNE; ran `scanpy.tl.umap` with parameter `random_state=0` to compute UMAP; ran `scanpy.tl.draw_graph` with parameters `random_state=0` and `iterations=5000` to compute FLE.

Pegasus. We ran `pegasus cluster` with parameters `-p 8 --knn-full-speed --diffmap --spectral-louvain --spectral-leiden --fitsne --net-umap --net-fle`.

2.5 Function calls, commands and parameters used for measuring Pegasus, SCANPY and Seurat v3 peak memory on the 5K PBMC and bone marrow datasets (Supplementary Table 7)

Seurat. For the 5K PBMC dataset, we first set `plan("multiprocess", workers=8)`. We then created a Seurat object by calling `CreateSeuratObject` with parameters `min.cells = floor(n.cells * 0.0005)` and `min.features = 500`, where `n.cells` represents total number of cell barcodes loaded. We then filtered any cells with fewer than 500 genes or more than 6,000 genes or with at least 20% of UMIs from mitochondrial genes. We next normalized data by calling `NormalizeData` with parameters `normalization.method = "LogNormalize"` and `scale.factor = 1e5`. Next, we ran `FindVariableFeatures` with parameters `mean.cutoff=c(0.0125, 7)` and `dispersion.cutoff=c(0.5, Inf)` for HVG selection; ran `ScaleData` with default parameters and `RunPCA` with `seed.use=0` for PCA computation; ran `FindNeighbors` with `k.param=100, dims=1:50` and `nn.method="annoy"` to find k neighbors; ran `FindClusters` with `resolution=1.3, random.seed=0` and `algorithm="louvain"` to find clusters using the Louvain algorithm; ran `RunTSNE` with `seed.use=0, dims=1:50` and `tsne.method="Fit-SNE"` to calculate tSNE-like visualization; ran `RunUMAP` with `seed.use=0, umap.method="umap-learn", metric="correlation", n.neighbors=15, min.dist=0.5 and dims=1:50` to calculate UMAP-like visualization. For the bone marrow dataset, we used the same procedure except the following changes: set `plan("multiprocess", workers=28)` and adjusted the threshold on mitochondrial rate to 10%.

SCANPY. For the 5K PBMC dataset, we first set `scanpy.settings.n_jobs=8`. We then filtered low quality cells by calling `scanpy.pp.filter_cells` four times with parameter settings `min_counts = 100, max_counts = 600000, min_genes = 500` and `max_genes = 6000` respectively. We then filtered low quality genes by calling `scanpy.pp.filter_genes` with parameter `min_cells = n.cells * 0.0005`, where `n.cells` is the total number of cells loaded. We also filtered cells with at least 20% mitochondrial rate. We normalized the data by calling `scanpy.pp.normalize_total` with parameter `target_sum = 1e5` and then calling `scanpy.pp.log1p`. Next, we ran `scanpy.pp.highly_variable_genes` with parameters `min_mean=0.0125, max_mean=7, min_disp=0.5` and `n_top_genes=2000` for HVG selection; ran `scanpy.pp.scale` with parameter `max_value=10` and then `scanpy.tl.pca` with parameter `random_state=0` to compute PCA; ran `scanpy.pp.neighbors` with parameters `n_neighbors=100` and `random_state=0` to find k neighbors; ran `scanpy.tl.diffmap` with parameter `n_comps=100` to compute diffusion map; ran `scanpy.tl.louvain` with parameters `resolution=1.3` and `random_state=0` for Louvain clustering; ran `scanpy.tl.tsne` with parameters `use_rep='X_pca', random_state=0` and `use_fast_tsne=True` to compute t-SNE; ran `scanpy.tl.umap` with parameter `random_state=0` to compute UMAP. For the bone marrow dataset, we used the same procedure except the following changes: set `scanpy.settings.n_jobs=28` and adjusted the threshold on mitochondrial rate to 10%.

Pegasus. For the 5K PBMC dataset, we ran `pegasus cluster` with parameters `-p 8 --percent-mito 20 --knn-full-speed --spectral-louvain --fitsne --net-umap`. For the bone marrow dataset, we ran `pegasus cluster` with parameters `-p 28 --knn-full-speed --spectral-louvain --fitsne --net-umap`.

2.6 Cloud benchmarking (Table 1)

For each of the three methods, we performed the following computational analyses: low quality cells/genes filtration, normalization to log expression space, HVG selection, batch correction, PCA, k-NN graph construction, clustering, tSNE-like and UMAP-like visualizations and find cluster-specific markers by differential

expression analysis. For Cumulus, we additionally ran a putative cell-type annotation step.

Seurat. The future framework is used for parallelization. We first filtered low quality cells and converted counts to log expression levels as described in the paper (using Seurat functions). Next, we ran `FindVariableFeatures` with parameters `selection.method="vst"`, `mean.cutoff=c(0.0125,7)`, `dispersion.cutoff=c(0.5, Inf)` and `nfeatures=2000`. To correct batch effects, we ran `FindIntegrationAnchors` with parameter `dims = 1:20` and `IntegrateData` with parameter `dims = 1:20`. In addition, we used only 2 threads for batch correction. We have tried 10, 15, 20 and 32 threads and they all failed. We then ran `ScaleData` with default parameters and `RunPCA` with `seed.use=0` and `npcs=50` for PCA computation; ran `FindNeighbors` with `reduction="pca"`, `dims=1:50`, `nn.method='annoy'`, `k.param=100` and `compute.SNN=TRUE` to find k neighbors; ran `FindClusters` with `resolution=1.3`, `random.seed=0` and `algorithm="louvain"` to compute clusters; ran `RunTSNE` with `seed.use=0`, `dims=1:50` and `tsne.method="Fit-SNE"` to calculate tSNE-like visualization; ran `RunUMAP` with `seed.use=0`, `umap.method="umap-learn"`, `metric="correlation"`, `n.neighbors=15` and `dims=1:50` to calculate UMAP-like visualization. Lastly, we ran `FindAllMarkers` with parameters `test.use="t"` and `random.seed=seed` to find cluster-specific markers.

SCANPY. We first set `scanpy.settings.n.jobs=os.cpu_count()`. Then we filtered low quality cells and converted counts to log expression levels as described in the paper (using SCANPY functions). Next, we ran `scanpy.pp.highly_variable_genes` with parameters `n_top_genes=2000` and `batch_key='Channel'` for HVG selection; ran `scanpy.pp.scale` with parameter `max_value=10` and then `scanpy.tl.pca` with parameters `n_comps=50`, `random_state=0` to compute PCA; imported `bbknn` python package directly and ran `bbknn.bbknn` with parameter `batch_key = 'Channel'` to correct batch effects; ran `scanpy.tl.louvain` with parameters `resolution=1.3` and `random_state=0` for Louvain clustering; ran `scanpy.tl.tsne` with parameters `use_rep='X_pca'`, `random_state=0` and `use_fast_tsne=True` to compute t-SNE; ran `scanpy.tl.umap` with parameter `random_state=0` to compute UMAP. Finally, we ran `scanpy.tl.rank_genes_groups` with parameters `groupby='louvain'` and `method='t-test'` to find cluster-specific markers.

Cumulus analysis step. We ran the Cumulus WDL with the following parameters: `zones="us-west1-b"`, `num.cpu=32`, `memory=120G`, `correct_batch_effect=true`, `minimum_number_of_genes=0`, `knn_full_speed=true`, `run_louvain=false`, `run_spectral_louvain=true`, `run_net_umap=true`, `cluster_labels=spectral_louvain_labels`, `auc=false`, `fisher=false` and `annotate_cluster=true`. In addition, since we did not compute diffusion maps, the spectral-Louvain was run on the principal component (PC) space.

References

- [1] K. Anand, G. Bianconi, and S. Severini. Shannon and von neumann entropy of random networks with heterogeneous expected degree. *Physical Review E*, 83(3):036109, 2011.
- [2] D. Calvetti, L. Reichel, and D. C. Sorensen. An implicitly restarted lanczos method for large symmetric eigenvalue problems. *Electronic Transactions on Numerical Analysis*, 2:1–21, 1994.
- [3] W. S. Cleveland, E. Grosse, and W. M. Shyu. *Statistical Models in S*, chapter Local Regression Models. Wadsworth & Brooks/Cole, 1992.
- [4] R. R. Coifman and S. Lafon. Diffusion maps. *Applied and Computational Harmonic Analysis*, 21(1):5–30, 2006.
- [5] L. Haghverdi, F. Buettner, and F. J. Theis. Diffusion maps for high-dimensional single-cell analysis of differentiation data. *Bioinformatics*, 31(18):2989–2998, 2015.
- [6] L. Haghverdi, M. Büttner, F. A. Wolf, F. Buettner, and F. J. Theis. Diffusion pseudotime robustly reconstructs lineage branching. *Nature Methods*, 13(10):845–848, 2016.
- [7] N. Halko, P. G. Martinsson, and J. A. Tropp. Finding structure with randomness: Probabilistic algorithms for constructing approximate matrix decompositions. *SIAM Review*, 53(2):217–288, 2011.
- [8] W. E. Johnson, C. Li, and A. Rabinovic. Adjusting batch effects in microarray expression data using empirical Bayes methods. *Biostatistics*, 8(1):118–127, 2007.
- [9] H. Kibirige. scikit-misc. *GitHub*, 2016. <https://github.com/has2k1/scikit-misc>.
- [10] C. Li and W. H. Wong. DNA-Chip Analyzer (dChip). In *Parmigiani G., Garrett E.S., Irizarry R.A., Zeger S.L. (eds) The Analysis of Gene Expression Data. Statistics for Biology and Health. Springer, New York, NY*, pages 120–141, 2003.
- [11] Y. A. Malkov and D. A. Yashunin. Efficient and robust approximate nearest neighbor search using Hierarchical Navigable Small World graphs. *IEEE Transactions on Pattern Analysis and Machine Intelligence*, 42(4):824–836, 2020.
- [12] K. R. Moon, D. van Dijk, Z. Wang, S. Gigante, D. B. Burkhardt, W. S. Chen, K. Yim, A. van den Elzen, M. J. Hirn, R. R. Coifman, N. B. Ivanova, G. Wolf, and S. Krishnaswamy. Visualizing structure and transitions in high-dimensional biological data. *Nature Biotechnology*, 37(12):1482–1492, 2019.
- [13] F. Pedregosa, G. Varoquaux, A. Gramfort, V. Michel, B. Thirion, O. Grisel, M. Blondel, P. Prettenhofer, R. Weiss, V. Dubourg, J. Vanderplas, A. Passos, D. Cournapeau, M. Brucher, M. Perrot, and E. Duchesnay. Scikit-learn: Machine learning in Python. *Journal of Machine Learning Research*, 12:2825–2830, 2011.
- [14] R. Satija, J. A. Farrell, D. Gennert, A. F. Schier, and A. Regev. Spatial reconstruction of single-cell gene expression data. *Nature Biotechnology*, 33(5):495–502, 2015.
- [15] T. Stuart, A. Butler, P. Hoffman, C. Hafemeister, E. Papalexi, W. M. I. Mauck, Y. Hao, M. Stoeckius, P. Smibert, and R. Satija. Comprehensive integration of single-cell data. *Cell*, 177(7):1888–1902.e21, 2019.
- [16] D. van Dijk, R. Sharma, J. Nainys, K. Yim, P. Kathail, A. J. Carr, C. Burdziak, K. R. Moon, C. L. Chaffer, D. Pattabiraman, B. Bierie, L. Mazutis, G. Wolf, S. Krishnaswamy, and D. Pe’er. Recovering gene interactions from single-cell data using data diffusion. *Cell*, 174(3):716–729.e27, 2018.
- [17] F. A. Wolf, P. Angerer, and F. J. Theis. SCANPY: Large-scale single-cell gene expression data analysis. *Genome Biology*, 19(1):15, 2018.
- [18] L. Zelnik-Manor and P. Perona. Self-tuning spectral clustering. In *NIPS’04 Proceedings of the 17th International Conference on Neural Information Processing Systems: Natural and Synthetic*, pages 1601–1608, 2004.